Role of depth and location of minima of a double-well potential on vibrational resonance

2010 J. Phys. A: Math. Theor. 43 465101

(http://iopscience.iop.org/1751-8121/43/46/465101)

IOP PUBLISHING JOURNAL OF PHYSICS A: MATHEMATICAL AND THEORETICAL

J. Phys. A: Math. Theor. **43** (2010) 465101 (11pp) doi:10.1088/1751-8113/43/46/465101

Role of depth and location of minima of a double-well potential on vibrational resonance

S Rajasekar[1], S Jeyakumari[2], V Chinnathambi[2] and M A F Sanjuan[3]

[1] School of Physics, Bharathidasan University, Tiruchirapalli 620 024, Tamilnadu, India
[2] Department of Physics, Sri KGS Arts College, Srivaikuntam 628 619, Tamilnadu, India
[3] Departamento de Física, Universidad Rey Juan Carlos, Tulipán s/n, 28933 Móstoles, Madrid, Spain

E-mail: rajasekar@cnld.bdu.ac.in

Received 8 June 2010, in final form 6 September 2010
Published 28 October 2010
Online at stacks.iop.org/JPhysA/43/465101

Abstract

We report our investigation into the role of depth and location of minima of a double-well potential on vibrational resonance in both underdamped and overdamped Duffing oscillators. The systems are driven by both low- and high-frequency periodic forces. We obtain theoretical expressions for the amplitude g of the high-frequency force at which resonances occur. The depth and location of the minima of the potential wells have a distinct effect on vibrational resonance in the underdamped and overdamped cases. In the underdamped system at least one resonance and at most two resonances occur and the number of resonances can be altered by varying the depth and location of the minima of the potential wells. We show that in the overdamped system there is always one and only one resonance, and the value of g at which resonance occurs is independent of the depth of the wells, but varies linearly with the locations of the minima of the wells.

PACS numbers: 05.45.-a, 05.90.+m, 46.40.Ff.

1. Introduction

The noise-induced stochastic resonance phenomenon can be of great use for low-frequency periodic signal detection. In a typical stochastic resonance, the signal-to-noise ratio (SNR) becomes maximum at an optimum noise strength. It has been shown that enhancement of response of a nonlinear system at the low-frequency of the input signal can be achieved when noise is replaced by a high-frequency periodic force and the associated resonance is termed as vibrational resonance [1, 2]. The analysis of vibrational resonance has received a considerable interest in recent years because of its importance in a wide variety of contexts in physics, engineering and biology. The occurrence of this resonance has been analysed theoretically

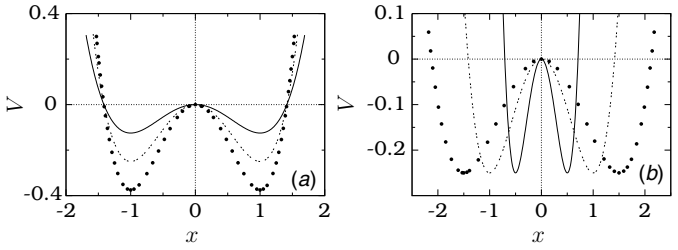

Figure 1. Shape of the potential $V(x)$ for $\omega_0^2 = \beta = 1$ and (a) $A = B = \alpha_1$ and (b) $A = \frac{1}{\alpha_2^2}$, $B = \frac{1}{\alpha_2^4}$. In the subplots, the values of $\alpha_1\,(a)$ and $\alpha_2\,(b)$ for continuous line, dashed line and painted circles are 0.5, 1 and 1.5, respectively.

[1–5], numerically [6–8] and experimentally [3, 5–11]. It has also been studied in a monostable [12], three wells [13] and asymmetric [14, 15] systems. From both theoretical and practical standpoints, it is of great importance to obtain an analytical estimate of control parameters at which vibrational resonance occurs. Along this direction, in a quintic oscillator, analytical expressions for control parameters at which vibrational resonance occurs are obtained using a theoretical approximation. Moreover, very recently, quasiperiodic vibrational resonance has been found in an overdamped bistable system with a time-delay feedback [16].

In this paper, we investigate the role of depth of the potential wells and the distance between the location of a minimum and local maximum of the symmetric double-well potential in both underdamped and overdamped Duffing oscillators on vibrational resonance. Interestingly, this goal can be achieved through a theoretical approach.

The equations of motion of the underdamped and overdamped systems are

$$\ddot{x} + \mathrm{d}\dot{x} + \frac{\mathrm{d}V(x)}{\mathrm{d}x} = f\cos\omega t + g\cos\Omega t, \tag{1}$$

and

$$\dot{x} + \frac{\mathrm{d}V(x)}{\mathrm{d}x} = f\cos\omega t + g\cos\Omega t, \tag{2}$$

respectively. We assume that $\Omega \gg \omega$. In equations (1) and (2) the potential $V(x)$ is

$$V(x) = -\tfrac{1}{2}A\omega_0^2 x^2 + \tfrac{1}{4}B\beta x^4. \tag{3}$$

For ω_0^2, β, A and $B > 0$ the potential $V(x)$ is of a symmetric double-well form. When $A = B = \alpha_1$ the potential has a local maximum at $x_0^* = 0$ and two minima at $x_\pm^* = \pm\sqrt{\frac{\omega_0^2}{\beta}}$. The depths of the left- and right-wells denoted by D_L and D_R, respectively, are same and equal to $\frac{\alpha_1\omega_0^4}{4\beta}$. By varying the parameter α_1 the depths of the two wells can be varied while keeping the values of $x_\pm^*$ unaltered. We call the underdamped system with $A = B = \alpha_1$ as US1. We call equation (1) with $A = \frac{1}{\alpha_2^2}$ and $B = \frac{1}{\alpha_2^4}$ as US2 in which case $x_0^* = 0$, whereas $x_\pm^* = \pm\alpha_2\sqrt{\frac{\omega_0^2}{\beta}}$ and $D_\mathrm{L} = D_\mathrm{R} = \frac{\omega_0^4}{4\beta}$ is independent of α_2. Thus, by varying α_2, the depth of the wells of $V(x)$ can be kept constant while the distance between the local maximum and the minima can be changed. We denote the overdamped version of the above two systems as OS1 and OS2, respectively. Figures 1(a) and (b) illustrate the effect of α_1 and α_2.

Systems (1) and (2) with $\alpha_1 = \alpha_2 = 1$ were considered by Blekhman and Landa [4]. They obtained the theoretical expression for response amplitude and shown the occurrence of resonances by varying the control parameters ω, g and Ω. They called the resonances observed

by varying the low-frequency ω and the high-frequency Ω as conjugate resonances. In this work we consider systems (1) and (2) with α_1 and α_2 arbitrary, obtain an analytical expression for the values of g at which resonance occurs, and analyse the effect of depth of the wells and the distance between the location of a minimum and local maximum of the potential $V(x)$ on resonance.

For $\Omega \gg \omega$, due to the difference in time scales of the low-frequency force $f\cos\omega t$ and the high-frequency force $g\cos\Omega t$, it is reasonable to assume that the solutions of systems (1) and (2) consist of a slow-motion $X(t)$ and a fast motion $\psi(t, \Omega t)$. For the underdamped and overdamped systems separately, we find an analytical expression for the response amplitude Q of the low-frequency (ω) output signal using a theoretical approach. From the expression of Q we obtain theoretical expressions for the values of g at which resonance occurs and analyse the effect of depth of the potential wells and the distance between the location of a minimum and local maximum of the symmetric double-well potential. We show that the number of resonances can be changed by varying the above two quantities in the underdamped systems. One or two resonances only can occur. One of the key results on the overdamped system (2) is that one and only one resonance is possible.

2. Underdamped systems

In this section we consider the underdamped systems US1 and US2. First, we obtain a theoretical expression for the response amplitude Q.

2.1. Theoretical approach

For $\Omega \gg \omega$ we assume that the solution of (1) consists of a slow-motion $X(t)$ with period $2\pi/\omega$ and a fast motion $\psi(t, \Omega t)$ with period $2\pi/\Omega$ (or period 2π in the fast time $\tau = \Omega t$). Substituting $x = X + \psi$ in equation (1) we obtain

$$\ddot{X} + \mathrm{d}\dot{X} - \left(A\omega_0^2 - 3B\beta\psi_{\mathrm{av}}^2\right)X + B\beta X^3 + B\beta\psi_{\mathrm{av}}^3 = f\cos\omega t, \tag{4}$$

where $\psi_{\mathrm{av}}^m = \frac{1}{2\pi}\int_0^{2\pi}\psi^m\,\mathrm{d}\tau$. In the equation for ψ, because ψ is a fast motion, we neglect $\dot{\psi}$, ψ, ψ^2 and ψ^3 and approximate it as $\ddot{\psi} = g\cos\Omega t$. From its solution we find $\psi_{\mathrm{av}} = \psi_{\mathrm{av}}^3 = 0$ and $\psi_{\mathrm{av}}^2 = \frac{g^2}{2\Omega^4}$. Then equation (4) takes the form

$$\ddot{X} + \mathrm{d}\dot{X} - C_1X + C_2X^3 = f\cos\omega t, \tag{5}$$

where

$$C_1 = A\omega_0^2 - \frac{3B\beta g^2}{2\Omega^4}, \qquad C_2 = B\beta. \tag{6}$$

The effective potential of (5) is

$$V_{\mathrm{eff}}(X) = -\tfrac{1}{2}C_1X^2 + \tfrac{1}{4}C_2X^4. \tag{7}$$

Slow oscillations occur about the equilibrium points $X_0^* = 0$, $X_\pm^* = \pm\sqrt{C_1/C_2}$. X_0^* is always an equilibrium point while $X_\pm^*$ exists only for $g < g_0 = \Omega^2\sqrt{\frac{2A\omega_0^2}{3B\beta}}$. That is, $V_{\mathrm{eff}}(X)$ remains as a double-well form for $g < g_0$ and becomes a single well for $g > g_0$.

Substituting $X = Y + X^*$, where Y is the deviation of slow motion from X^*, in equation (5), in the linear approximation for $f \ll 1$ we have $Y(t) = A_{\mathrm{L}}\cos(\omega t + \phi)$, where

$$A_{\mathrm{L}} = \frac{f}{\sqrt{\left(\omega_{\mathrm{r}}^2 - \omega^2\right)^2 + \mathrm{d}^2\omega^2}}, \qquad \phi = \tan^{-1}(\omega/C_1), \tag{8}$$

where the resonant frequency is given by

$$\omega_{\rm r}^2 = -A\omega_0^2 + \frac{3B\beta g^2}{2\Omega^4} + 3B\beta X^{*2}. \tag{9}$$

The response amplitude is $Q = A_{\rm L}/f$.

2.2. Role of depth of the potential wells on vibrational resonance

The possibility of occurrence of resonance when a control parameter is varied and the values of the parameter at which resonance occurs can be determined from the theoretical expression of Q. We note that Q is maximum when $S = \left(\omega_{\rm r}^2 - \omega^2\right)^2 + {\rm d}^2\omega^2$ becomes a minimum. When g is treated as a control parameter, vibrational resonance occurs at $g = g_{\rm VR}$ where $g_{\rm VR}$ is a root of the equation

$$S_g = \frac{{\rm d}S}{{\rm d}g} = 4\left(\omega_{\rm r}^2 - \omega^2\right)\omega_{\rm r}\omega_{{\rm r}g} = 0, \tag{10}$$

where $\omega_{{\rm r}g} = \frac{{\rm d}\omega_{\rm r}}{{\rm d}g}$. For US1 with $A = B = \alpha_1$ we obtain

$$g_{\rm VR}^{(1)} = \Omega^2\left[\frac{2\omega_0^2}{3\beta} - \frac{\omega^2}{3\alpha_1\beta}\right]^{1/2}, \qquad \alpha_1 > \alpha_{1{\rm c}} = \frac{\omega^2}{2\omega_0^2}, \tag{11}$$

$$g_{\rm VR}^{(2)} = \Omega^2\left[\frac{2\omega_0^2}{3\beta} + \frac{2\omega^2}{3\alpha_1\beta}\right]^{1/2}, \qquad \alpha_1 - \text{arbitrary}. \tag{12}$$

Equation (12) implies that there is always one resonance for any value of $\alpha_1 > 0$ at $g = g_{\rm VR}^{(2)}$. Another resonance occurs only for $\alpha_1 > \alpha_{1{\rm c}}$ at $g = g_{\rm VR}^{(1)}$ and $g_{\rm VR}^{(1)} < g_{\rm VR}^{(2)}$. In terms of the depth $D_{\rm L}$ $(= D_{\rm R})$ of the potential wells the condition for double resonance is $D_{\rm L} > \frac{\omega_0^2\omega^2}{8\beta}$. The number of resonances and the value of $g_{\rm VR}$ can be controlled by varying the parameter α_1, that is, the depth of the two wells of the potential. Further, as ω increases $g_{\rm VR}^{(1)}$ decreases while $g_{\rm VR}^{(2)}$ increases. The separation between the two resonances increases with an increase in ω. As α_1 increases from $\alpha_{1{\rm c}}$, $g_{\rm VR}^{(1)}$ increases while $g_{\rm VR}^{(2)}$ decreases. The separation between the two resonances decreases with an increase in α_1. That is, ω and α_1 have opposite effects. In the limit $\alpha_1 \to \infty$, $g_{\rm VR}^{(1)}$ and $g_{\rm VR}^{(2)} \to \Omega^2\sqrt{\frac{2\omega_0^2}{3\beta}}$.

The above theoretical predictions are verified numerically. From the numerical solution $x(t)$ the response amplitude Q is computed through $Q = \sqrt{Q_{\rm S}^2 + Q_{\rm C}^2}/f$ where

$$Q_{\rm S} = \frac{2}{nT}\int_0^{nT} x(t)\sin\omega t\,{\rm d}t, \tag{13a}$$

$$Q_{\rm C} = \frac{2}{nT}\int_0^{nT} x(t)\cos\omega t\,{\rm d}t, \tag{13b}$$

where $T = 2\pi/\omega$ and n is taken as 500. We fix the values of the parameters in US1 and US2 as $\omega_0^2 = \beta = 1$, $d = 0.5$, $\omega = 1$, $\Omega = 10$ and $f = 0.05$.

Figure 2(*a*) presents theoretical and numerical $g_{\rm VR}$ versus α_1. Theoretical $g_{\rm VR}$ is in very good agreement with the numerical $g_{\rm VR}$. To understand the mechanism of single and double resonances, in figure 2(*b*) we plot the resonant frequency $\omega_{\rm r}$ as a function of g for four values of α_1. For each fixed value of α_1 as g increases from 0 the resonant frequency $\omega_{\rm r}$ decreases from the value $\sqrt{2\alpha_1\omega_0^2}$ and $\to 0$ as $g \to g_0 = \Omega^2\sqrt{\frac{2\omega_0^2}{3\beta}} = 81.65$. The value of $g(= g_0)$ at

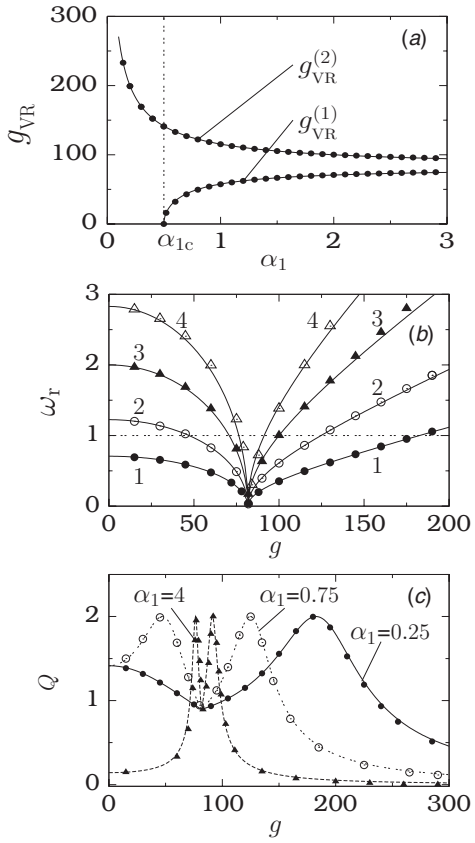

Figure 2. (*a*) Plot of $g_{\rm VR}$ as a function of the parameter α_1 in US1. Continuous lines are theoretical $g_{\rm VR}$ while the painted circles are numerically computed $g_{\rm VR}$. (*b*) Variation of theoretical (represented by continuous lines) and numerically computed (represented by symbols) resonant frequencies with g. Numerical resonant frequency is calculated using the numerical solution of equation (1). Labels 1–4 correspond to $\alpha_1 = 0.25$, 0.75, 2 and 4, respectively. The horizontal dashed line represents $\omega_{\rm r} = \omega = 1$. (*c*) Response amplitude Q versus g for three values of α_1. The theoretical and numerical values of Q are represented by curves and symbols respectively. Theoretically predicted values of $g_{\rm VR}$, $\omega_{\rm r}$ and Q are in good agreement with the respective values obtained in numerical simulation.

which $V_{\rm eff}$ undergoes bifurcation from a double well to a single well is independent of α_1. For $g > g_0$, $V_{\rm eff}$ becomes a single-well potential and $\omega_{\rm r}$ increases with increase in g. Resonance will take place whenever $\omega_{\rm r} = \omega$. In figure 2(*b*) for $\alpha_1 = 0.25 < \alpha_{1c} = 0.5$ the $\omega_{\rm r}$ curve intersects the $\omega = 1$ dashed line at only one value of $g > g_0$. In figure 2(*c*) we notice only one resonance for $\alpha_1 = 0.25$. For $\alpha_1 > \alpha_{1c}$ the $\omega_{\rm r}$ curve intersects the $\omega = 1$ line at two values of g: one below g_0 and another above g_0. This is shown in figures 2(*b*) and (*c*) for few values of α_1. Because the resonance observed in our study is due to the high-frequency force it is referred as vibrational resonance. The vibrational resonance can be observed either by varying the amplitude g or the frequency Ω of the force $g\cos\Omega t$.

Now, we compare the slow-motion $X(t)$ described by equation (5) and the actual motion $x(t)$ of the system (1). In equation (5), the coefficient of the linear term X depends on both amplitude g and the frequency Ω of the high-frequency force. The number of equilibrium points and their locations about which slow oscillations occur can be altered by varying g or

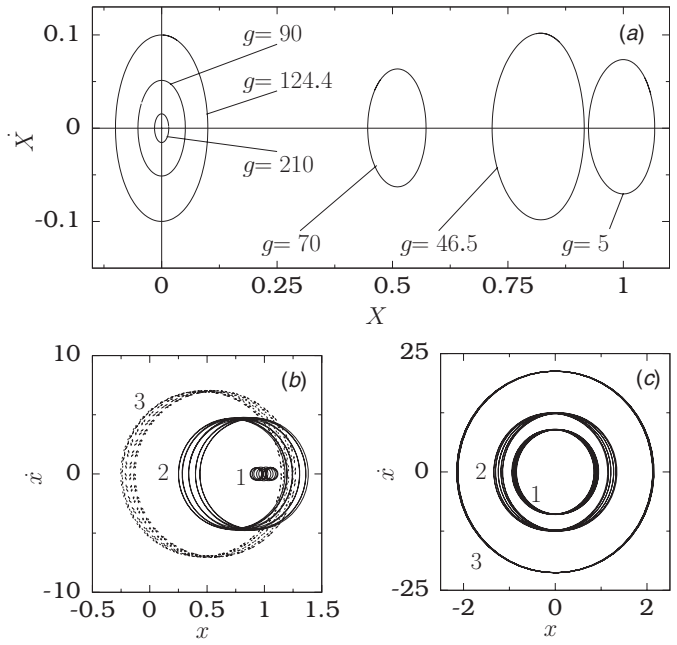

Figure 3. Phase portraits of (*a*) slow motion and (*b*)–(*c*) actual motion of the system (1) for several values of g. In the subplot (*b*) the values g for the orbits marked by 1, 2 and 3 are 5, 46.5 and 70, respectively. In (*c*) the values of g for the orbits marked by 1, 2 and 3 are 90, 124.4 and 210 respectively. All the orbits are periodic with period $2\pi/\omega$. The value of α_1 is 0.75.

Ω. For $g < g_0 = 81.65$, equation (5) has two coexisting orbits one about X^*_+ and another about X^*_-. As g increases $X^*_\pm$ move towards $X^*_0 = 0$ and consequently the slow orbits also move toward the origin. This is clear from the phase portrait of the orbits shown in figure 3(*a*) for $\alpha_1 = 0.75$ and $g = 5$, 46.5 and 70. (The orbits in the region $X < 0$ are not shown in figure 3(*a*)). Further, we note that the amplitude of $X(t)$ is maximum for $g = g_{\rm VR} = 46.5$. In figure 3(*b*) the actual motions corresponding to $g = 5$, 46.5 and 70 are shown. For $g = g_{\rm VR} = 46.5$ there is no cross-well motion of systems (1) and (5). For $g > g_0$, the effective potential $V_{\rm eff}$ becomes a single-well form and the slow motion takes place about $X^*_0 = 0$ and the actual motion $x(t)$ also occurs about $x^*_0 = 0$. This is illustrated in figures 3(*a*) and (*c*) for $g = 90$, 124.4 (at which second resonance occurs) and 210. As g increases, the size of the slow orbit increases, becomes maximum at $g = g_{\rm VR}$ and then decreases, whereas the size of the orbit of the system (1) increases continuously with an increase in g.

2.3. Role of location of minima of the potential on vibrational resonance

For US2 with $A = 1/\alpha_2^2$ and $B = 1/\alpha_2^4$, as α_2 increases the location of the two minima of $V(x)$ move away from the origin in the opposite direction, i.e. the distance between a minimum and the local maximum $x^*_0 = 0$ of the potential increases with increase in α_2. We find

$$g^{(1)}_{\rm VR} = \Omega^2\alpha_2\left[\frac{2\omega_0^2}{3\beta} - \frac{\alpha_2^2\omega^2}{3\beta}\right]^{1/2}, \qquad \alpha_2 < \alpha_{2c} = \sqrt{\frac{2\omega_0^2}{\omega^2}}, \tag{14}$$

$$g^{(2)}_{\rm VR} = \Omega^2\alpha_2\left[\frac{2\omega_0^2}{3\beta} + \frac{\alpha_2^2\omega^2}{3\beta}\right]^{1/2}, \qquad \alpha_2 - \text{arbitrary}. \tag{15}$$

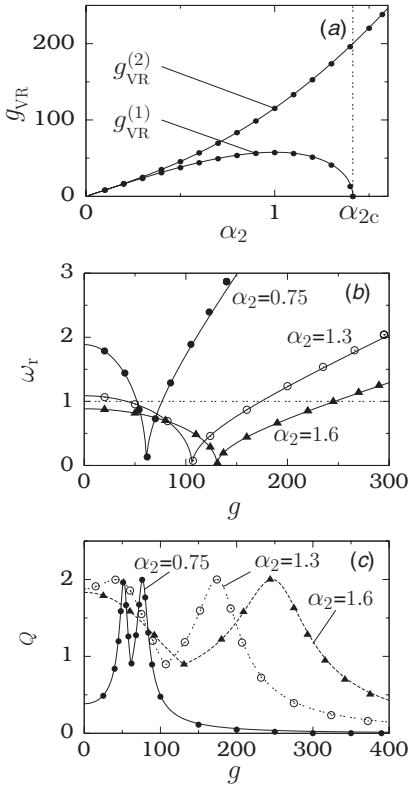

Figure 4. (*a*) $g_{\rm VR}$ versus α_2 in US2 where α_2 characterizes the distance between the maximum $x_0^* = 0$ and the minima $x_\pm^*$ of the potential. Continuous lines are theoretical $g_{\rm VR}$ while the painted circles are numerically computed $g_{\rm VR}$. (*b*) Theoretical resonant frequency $\omega_{\rm r}$ (marked by continuous lines) and numerically computed $\omega_{\rm r}$ (marked by symbols) versus g for three values of α_2. The horizontal dashed line represents $\omega_{\rm r} = \omega = 1$. (*c*) Q versus g for three values of α_2. The theoretical and numerical values of Q are represented by curves and symbols, respectively.

Figure 4(*a*) depicts both theoretical and numerical $g_{\rm VR}$ versus α_2. The difference in the effect of the distance of $x_\pm^*$ from origin over the depth of the potential wells can be seen by comparing figure 4(*a*) with figure 2(*a*). In US1 two resonances occur above a certain critical depth (α_{1c}) of the wells. In contrast to this, in US2 two resonances occur only for $\alpha_2 < \alpha_{2c}$ or in terms of $x_\pm^*$, $x_\pm^* < x_c^* = \frac{\omega_0^2}{\omega}\sqrt{\frac{2}{\beta}}$. For $\omega_0^2 = \beta = \omega = 1$, the values chosen in our numerical study are, $x_c^* = \sqrt{2}$ and $\alpha_{2c} = \sqrt{2}$. (If $\beta \neq 1$, then $x_c^* \neq \alpha_{2c}$). From equation (14) we infer that as α_2 increases from a small value (i.e. as $x_\pm^*$ moves away from origin), $g_{\rm VR}^{(1)}$ increases and reaches a maximum value $\frac{\Omega^2\omega_0^2}{\sqrt{3\beta\omega}}$ at $\alpha_2 = \frac{\sqrt{\omega_0^2}}{\omega}$. Then with further increase in α_2, it decreases and $\to 0$ as $\alpha_2 \to \alpha_{2c}$. We note that $g_{\rm VR}^{(2)}$ of US1 decreases with an increase in α_1, while $g_{\rm VR}^{(2)}$ of US2 increases with an increase in α_2. Figure 4(*b*) shows the variation of $\omega_{\rm r}$ with g for three values of α_2. Theoretical $\omega_{\rm r} = 0$ at $g = g_0 = \Omega^2\alpha_2\sqrt{\frac{2\omega_0^2}{3\beta}}$. The bifurcation point g_0 increases linearly with α_2. Sample response curves for three fixed values of α_2 are shown in figure 4(*c*). In the double-resonance case the separation between the two resonances increases with an increase in α_2. The converse effect is noticed in US1.

In US1 and US2, the resonances are due to the minimization of the function S which occurs when the resonant frequency ω_r matches with the low-frequency ω of the input signal $f\cos\omega t$. Consequently, at resonance $Q = Q_{max} = \frac{1}{d\omega}$ and it depends only on d and ω. Since $d = 0.5$ and $\omega = 1$ in figures 2(c) and 4(c) at resonance $Q = 2$. Equation (10) indicates that resonance can occur when $\omega_{rg} = 0$. However, for the symmetric double-well systems considered in this work, we find that $\omega_{rg} \neq 0$ for any nonzero value of g. A resonance due to $\omega_{rg} = 0$ is found in the monostable and multistable quintic oscillator [12, 13].

It is noteworthy to compare the high-frequency-induced vibrational resonance with the noise-induced stochastic resonance [17, 18]. In a typical noise driven double-well system, the SNR increases with an increase in the noise intensity, reaches a maximum value and then decreases with further increases in the noise intensity. Stochastic resonance occurs when the motion exhibits periodic switching between the two wells. Further, only one stochastic resonance is observed. It does not occur in monostable systems with additive Gaussian noise. When the noise term is replaced by a high-frequency force, $g\cos\Omega t$, the response amplitude Q becomes maximum at one or more values of g depending on the values of other parameters. Vibrational resonance can occur without cross-well motion. This is because, as seen from the theoretical expression of the response amplitude Q, the mechanism of vibrational resonance matches of the resonant frequency ω_r with the low-frequency ω of the input signal $f\cos\omega t$.

2.4. Validity of theoretical prediction

It has been pointed out [4, 5] that for parametric values near the transition from bistability to monostability, a nonlinear system becomes highly sensitive to external perturbations such as a periodic driving force. Moreover, in system (1) as $g \to g_0$ (the bifurcation point), the resonant frequency $\omega_r \to 0$. As a result of these, a considerable deviation of theoretical response amplitude Q with the numerical Q is found for small values of ω for values of g near the bifurcation value g_0. For small values of ω theoretical Q is in good agreement with the numerical Q for values of g far before and far after g_0. We study the effect of ω, ω_0^2 and d on theoretical Q for a wide range values of g in US1. Results similar to US1 are also observed in US2.

In figure 5(a) both theoretical Q and numerical Q are plotted as a function of ω for four values of g. Here $g_0 = 81.65$. For $g = 60$ and 100, the values far from g_0, theoretical and numerical Q are very close. When $g = 75$ and 90, the values close to g_0, the deviation of theoretical Q from numerical Q is large for $\omega < 0.4$. Figure 5(b) shows g versus Q for $\omega = 1$, 0.4 and 0.2. For $\omega = 1$, the theory predicts double resonance at $g = g_{VR} = 47.1$ and 124.7, while in the numerical simulation resonance is observed at $g = 46.5$ and 124.4. These values of g_{VR} are far from $g_0 = 81.65$. For $\omega = 0.2$, the theory gives $g_{VR} = 80.55$ and 83.80 and are close to g_0, while numerically only one resonance at $g = 76.85$ is noticed. Moreover, for values of g near g_0, the discrepancy between theory and numerical is considerably large. In order to know whether the discrepancy is mainly because of $\omega = 0.2 \ll \omega_0^2 = 1$, we plotted g versus Q for $\omega_0^2 = 1$ and 0.2 for $\omega = 0.2$ in figure 5(c). Even for $\omega_0^2 = \omega = 0.2$, the deviation of theoretically predicted Q from numerically computed Q is large for values of g near $g_0(= 36.51)$. The discrepancy between theory and numerical simulation can be reduced by increasing the value of the damping coefficient d. This is shown in figure 5(d). For $d = 1$ and 2, the theoretical response amplitude is very close to the numerically computed response amplitude, however, the value of $Q_{max}(g = g_{VR})$ is reduced by increasing the value of d. In figures 2(c), 4(c) and 5 we notice close agreement between theoretical Q and numerically computed Q when Q_{max} is roughly <3. From the above analysis, we point out that in practical applications of theoretical treatment of vibrational resonance it is appropriate

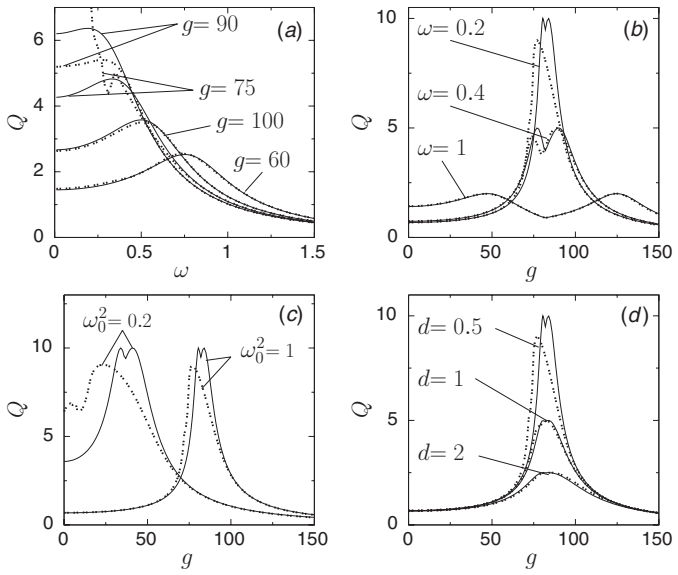

Figure 5. (*a*) ω versus theoretical Q (marked by continuous lines) and numerical Q (marked by dotted lines) for four fixed values of g for US1. Here $\omega_0^2 = 1$, $\beta = 1$, $d = 0.5$, $f = 0.05$, $\Omega = 10$ and $\alpha_1 = 0.75$. (*b*)–(*d*) g versus Q. (*b*) $\omega = 0.2$, 0.4 and 1; (*c*) $\omega_0^2 = 0.2$ and 1 with $\omega = 0.2$; (*d*) $d = 0.5$, 1 and 2 with $\omega = 0.2$ and $\omega_0^2 = 1$.

to avoid $Q_{\max} \gg 1$ and choose values of the parameters for which $Q_{\max}$ is say < 3. This is particularly important for small values of ω.

The actual motions of equations (1) and (5) are studied for the parametric choices considered in figure 5. Figure 6 shows the bifurcation diagrams of equation (5). We restricted our analysis to the range $0 < g < 400$. For $\omega = 0.4$, the period-T solution is found (figure 6(*a*)) in the above range of g. When $\omega = 0.2$, chaotic motion and other periodic orbits are found for $g \in [72.24, 73.6]$, an interval of g near $g_0 = 81.65$. This is shown in figure 6(*b*). Orbits other than the period-T orbit (assumed in the theoretical analysis) are found near $g_0 = 36.51$ for $\omega_0^2 = \omega = 0.2$ (figure 6(*c*)). In figure 6(*d*), corresponding to the parametric choices of figure 5(*d*) with $d = 1$, the period-T solution assumed in the theoretical treatment is also observed in the numerical simulation and other periodic and chaotic motions are not found. Results similar to the above are found in solving equation (1) numerically.

3. Overdamped systems

For overdamped systems, equation (2), the response amplitude Q is obtained as

$$Q = \frac{1}{\sqrt{\omega_{\rm r}^2 + \omega^2}}, \tag{16}$$

where

$$\omega_{\rm r}^2 = -A\omega_0^2 + \frac{3B\beta g^2}{2\Omega^2} + 3B\beta X^{*2}. \tag{17}$$

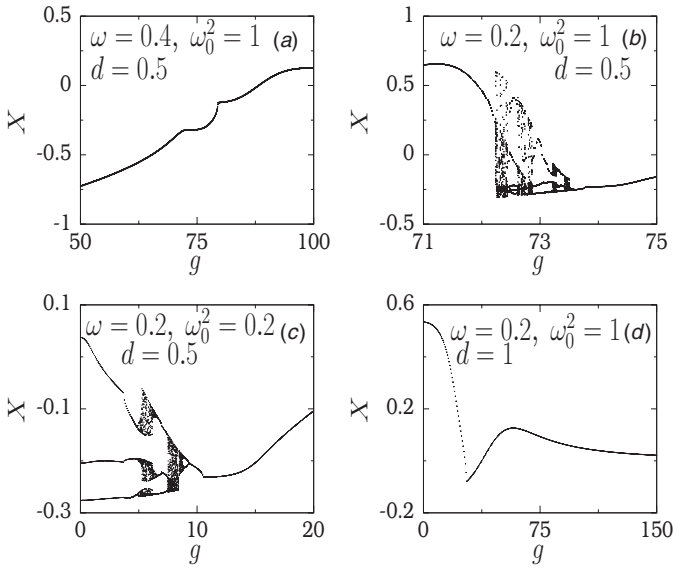

Figure 6. Bifurcation diagrams of equation (5) near g_0. The values of X are collected at $t = n \times (2\pi/\omega)$, $n = 1, 2, \ldots, 200$ after leaving sufficient transient motion. The values of the parameters are $f = 0.05$, $\Omega = 10$, $\beta = 1$, $\alpha_1 = 0.75$ and (*a*) $\omega = 0.4$, $\omega_0^2 = 1$, $d = 0.5$, (*b*) $\omega = 0.2$, $\omega_0^2 = 1$, $d = 0.5$, (*c*) $\omega = \omega_0^2 = 0.2$, $d = 0.5$ and (*d*) $\omega = 0.2$, $\omega_0^2 = 1$, $d = 1$. For $\omega_0^2 = 1$ and 0.2 the values of g_0 are 81.65 and 36.51, respectively.

Q is maximum when $\omega_r = 0$. For OS1 ($A = B = \alpha_1$) and OS2 $\left(A = 1/\alpha_2^2,\ B = 1/\alpha_2^4\right)$ we have

$$\text{OS1}: \ g_{\text{VR}} = \Omega\sqrt{\frac{2\omega_0^2}{3\beta}}, \qquad \text{OS2}: \ g_{\text{VR}} = \Omega\alpha_2\sqrt{\frac{2\omega_0^2}{3\beta}}. \tag{18}$$

There are several interesting results:

- The most significant result is that g_{VR} of OS1 is independent of the depth of the wells of the symmetric double-well potential;
- g_{VR} of OS1 is $(1/\Omega)$ times the limiting value (in the limit of $\alpha_1 \to \infty$ in equations (11) and (12)) of US1;
- g_{VR} of OS2 is α_2 times the g_{VR} of OS1. Because g_{VR} of OS2 with $\alpha_2 < 1$ is lower than g_{VR} of OS1, the former is advantageous compared to the latter;
- In OS1 and OS2 there is always one and only one vibrational resonance;
- g_{VR} of OS1 and OS2 corresponds to the value of g at which the effective potential $V_{\text{eff}}(X)$ undergoes bifurcation from double well to a single well. In US1 and US2 resonance does not occur at the bifurcation point $g = g_0$.

In OS1 and OS2 also discrepancy between theoretical and numerical predictions is observed for small values of ω near $g = g_0$.

4. Conclusions

In summary, using a theoretical approach we analysed the effect of depth of the wells and the distance of a minimum and the local maximum of the double-well potential of the Duffing

oscillators (1) and (2). These two quantities have distinct effects. The dependence of g_{VR} on these quantities are explicitly determined. The number of resonances and the value of g_{VR} can be controlled by varying the parameters α_1 and α_2. $Q_{\max}$ is independent of α_1 and α_2 in the four systems. g_{VR} of OS1 is independent of α_1 while in US1 it depends on α_1. g_{VR} of OS2 varies linearly with α_2 whereas in US2 it is a nonlinear function of α_2. In the overdamped systems only one resonance occurs. Double resonance is possible in US1 and US2 for certain range of values of α_1 and α_2, respectively. We have discussed the effect of ω, ω_0^2 and d on theoretical Q near the bifurcation point g_0.

Vibrational resonance has been studied in the overdamped bistable system with the asymmetric potential $V(x) = -\frac{1}{2}\alpha x^2 + \frac{1}{4}\beta x^4 - \gamma x$, α, β, $\gamma > 0$ [15] and with $V(x) = 4(x - x^3) + \Delta$ [11], where Δ is a constant parameter describing the level of asymmetry. Single resonance is reported when the amplitude of the high-frequency force or Δ is varied. It is possible to realize experimentally double-well Duffing oscillators where (i) the depth of the right-well remains same while the depth of the left-well can be altered and (ii) the location of the right-well local minimum remains same while the local minimum of left-well can be altered. It is of interest to analyse the effect of difference in the depths and the locations of the minima of the wells on vibrational resonance.

Acknowledgments

The authors are grateful to the referees for their suggestions which improved the quality and presentation of this paper. MAFS acknowledges financial support from the Spanish Ministry of Education and Science under Project no. FIS2006-08525 and from the Spanish Ministry of Science and Innovation under Project no. FIS2009-09898.

References

[1] Landa P S and McClintock P V E 2000 *J. Phys. A: Math. Gen.* **33** L433
[2] Gittermann M 2001 *J. Phys. A: Math. Gen.* **34** L355
[3] Baltanas J P, Lopez L, Blekhman I I, Landa P S, Zaikin A, Kurths J and Sanjuan M A F 2003 *Phys. Rev.* E **67** 066119
[4] Blekhman I I and Landa P S 2004 *Int. J. Nonlinear Mech.* **39** 421
[5] Chizhevsky V N 2008 *Int. J. Bifurcation Chaos* **18** 1767
[6] Ullner E, Zaikin A, Garcia-Ojalvo J, Bascones R and Kurths J 2003 *Phys. Lett.* A **312** 348
[7] Deng B, Wang J and Wei X 2009 *Chaos* **19** 013117
[8] Deng B, Wang J, Wei X, Tsang K M and Chan W L 2010 *Chaos* **20** 013113
[9] Chizhevsky V N and Giacomelli G 2004 *Phys. Rev.* E **70** 062101
[10] Chizhevsky V N and Giacomelli G 2005 *Phys. Rev.* A **71** 011801(R)
[11] Chizhevsky V N and Giacomelli G 2008 *Phys. Rev.* E **77** 051126
[12] Jeyakumari S, Chinnathambi V, Rajasekar S and Sanjuan M A F 2009 *Phys. Rev.* E **80** 046608
[13] Jeyakumari S, Chinnathambi V, Rajasekar S and Sanjuan M A F 2009 *Chaos* **19** 043128
[14] Chizhevsky V N, Smeu E and Giacomelli G 2003 *Phys. Rev. Lett.* **91** 220602
[15] Chizhevsky V N and Giacomelli G 2006 *Phys. Rev.* E **73** 022103
[16] Yang J H and Liu X B 2010 *J. Phys. A: Math. Theor.* **43** 122001
[17] Jung P 1993 *Phys. Rep.* **234** 175
[18] Gammaitoni L, Hanggi P, Jung P and Marchesoni F 1998 *Rev. Mod. Phys.* **70** 223